Author Manuscript

Author Manuscript

Author Manuscript

Author Manuscript

HHS Public Access

Author manuscript

*Nature*. Author manuscript; available in PMC 2014 April 17.

Published in final edited form as:

*Nature*. 2013 May 2; 497(7447): 74–79. doi:10.1038/nature12112.

# Hippocampal place cell sequences depict future paths to remembered goals

**Brad E Pfeiffer**[1] and **David J Foster**[1,*]

[1]Solomon H Snyder Department of Neuroscience, Johns Hopkins University School Of Medicine, Baltimore, MD 21205, USA

## Abstract

Effective navigation requires planning extended routes to remembered goal locations. Hippocampal place cells have been proposed to play a role in navigational planning but direct evidence has been lacking. Here, we show that prior to goal-directed navigation in an open arena, the hippocampus generates brief sequences encoding spatial trajectories strongly biased to progress from the subject's current location to a known goal location. These sequences predict immediate future behavior, even in cases when the specific combination of start and goal locations is novel. These results suggest that hippocampal sequence events previously characterized in linearly constrained environments as 'replay' are also capable of supporting a goal-directed, trajectory-finding mechanism, which identifies important places and relevant behavioral paths, at specific times when memory retrieval is required, and in a manner which could be used to control subsequent navigational behavior.

---

A fundamental purpose of memory lies in utilizing previous experience to inform current choices, directing behavior toward reward and away from negative consequences based upon knowledge of prior outcomes in similar situations. Goal-directed spatial navigation – planning extended routes to remembered locations – requires both memory of the goal location and knowledge of the intervening terrain in order to determine an efficient and safe path. The hippocampus has long been known to play a critical role in spatial memory[1,2] and memory for events[3,4], and it has been proposed that the hippocampus might play a fundamental role in calculating routes to goals, especially under conditions demanding behavioral flexibility[1,5–8]. This proposal stems largely from the discovery that excitatory neurons of the hippocampus exhibit spatially localized place responses during exploration[1]. However, it has been a challenge to understand how individual place responses tied to the current location might be informative about other locations that the animal cares about, such as the remembered goal[9], or the set of locations defining a route[10,11].

---

Users may view, print, copy, download and text and data- mine the content in such documents, for the purposes of academic research, subject always to the full Conditions of use: http://www.nature.com/authors/editorial_policies/license.html#terms

*Correspondence and requests for materials should be addressed to D.J.F. (david.foster@jhu.edu).

Supplementary Information is linked to the online version of the paper at www.nature.com/nature.

**Author Contributions:** B.E.P. and D.J.F. designed the experiment and analyses, B.E.P. collected the data, B.E.P. and D.J.F. wrote the paper.

**Author Information:** Reprints and permissions information is available at npg.nature.com/reprintsandpermissions. The authors declare no competing financial interests.

Author Manuscript Author Manuscript Author Manuscript Author Manuscript

That place cells systematically represent positions other than the current location has been revealed through the use of techniques to record simultaneously from multiple hippocampal place cells[12]. The early discovery of phase precession of place cell spikes relative to theta frequency oscillations in the local field potential (LFP)[13] led to the hypothesis that place cells fire in sequences within a theta cycle, and thus represent places behind or ahead of the animal [14–16]. Theta sequences have since been demonstrated experimentally across place cell populations[17]. Also during theta, place cell activity appears to "sweep" ahead of an animal located at a choice point[18], leading to the hypothesis that such activity could support the evaluation of alternatives during decision making[19]. A separate group of phenomena termed "replay" has been found during sleep[20,21] and non-exploratory awake periods[22], and is associated with sharp-wave-ripple (SWR) events in the hippocampal LFP (with the sole exception of replay during REM sleep[20]). In replay, simultaneously recorded populations of place cells exhibit reactivation of temporal sequences reflecting prior behavioral trajectories up to 10m long[23]. While these forms of non-local activity are now well established[17,23–26], it has proven difficult to establish a predictive relationship between non-local place cell activity and behavior[18,26], because of the two-fold technical problem of ensuring adequate behavioral sampling of the environment while recording from sufficient numbers of place cells. Thus it remains unknown whether non-local place cell activity can specify remembered goals, or define specific routes that the animal will take.

## Hippocampal ensembles encode two-dimensional trajectories

We recorded from hippocampal neurons while rats performed a spatial memory task, using the statistical power of an open field design in which the goal was one of 36 clearly separated locations within a 2m x 2m arena (Fig 1a). We addressed the sampling problem by combining random foraging and goal-directed behavior, and by implanting miniaturized lightweight microdrives supporting 40 independently adjustable tetrodes, with 20 tetrodes targeted to each dorsal hippocampal area CA1 (Sup Fig 1), to record simultaneously from up to 250 hippocampal neurons with well defined place fields. Our task, incorporating elements from previous task designs[9,27–29], was composed of trials each consisting of two phases: In phase one, the rat was required to forage to obtain reward (liquid chocolate) in an unknown location (*RANDOM*). In phase two, the rat could obtain reward in a predictable reward location (*HOME*). The transition to the next phase or trial was automatic upon consummation of the reward, and was not signaled to the animal. The task incorporated several features. First, because the shortest routes in phase one and two were matched, it was determined that animals could remember *HOME*, but could not detect *RANDOM* locations, since latencies and path lengths were significantly shorter for *HOME* bound trajectories (Figs 1b–d). Second, the *HOME* location was moved to a novel location each day. Thus, animals were required to learn a new goal location, demanding a flexible behavioral response that was more likely to engage the hippocampus than a fixed reference-memory response [27,30,31]. Third, for the first 19 trials of each day, the *RANDOM* locations were non-repeating. Hence during this period, every *HOME*-bound trajectory was always a novel combination of current location and goal location. Thus, our task probed both memory for the goal location and flexible planning of a novel route to get there.

Author Manuscript Author Manuscript Author Manuscript Author Manuscript

We implanted four well-trained rat subjects with the 40-tetrode microdrive for electrophysiological recording. Large numbers of well-isolated units (Sup Fig 2) [32] were recorded simultaneously during behavioral sessions on two consecutive days (212 and 250 units active during exploration from rat 1 on experimental days 1 and 2, respectively; 166 and 193 units from rat 2 on days 1 and 2; 133 and 106 units from rat 3 on days 1 and 2; 103 and 175 units from rat 4 on days 1 and 2). The recorded units demonstrated position-specific firing patterns ("place fields") that were distributed throughout the environment (Sup Figs 3–5), and a memory-less, uniform prior Bayesian decoding algorithm[23] allowed us to estimate the spatial location of the rat accurately from the recorded spike trains throughout the experiment (Sup Fig 6; Sup Video 1). We identified candidate events as brief increases in population spiking activity during periods of immobility while the rat performed the task (Fig 2a) and applied the decoding algorithm to the population spike trains (Fig 2b). During many candidate events, decoded position revealed temporally compressed, two-dimensional trajectories across the environment (Fig 2c; Sup Video 2). We applied length, duration and smoothness criteria to the decoded positions of candidate events to define "trajectory events" (see methods). We found between 144 and 373 trajectory events per session (between 25.3% and 43.9% of candidate events) with a mean duration of 103.6 ms, and path lengths that ranged from 40.0 cm to 199.1 cm (Sup Fig 7; Sup Table 1). We tested the probability that trajectory events could have occurred by chance, using two separate Monte-Carlo shuffle methods which varied either cell identity or place field position (see methods). Zero (out of 2028) trajectory events had a *P*-value greater than 0.02 under either method, indicating that all trajectory events were statistically significant events. Spectrogram analysis of trajectory events strongly matched SWR events identified within the same experimental sessions (Sup Fig 8a). In addition, an overwhelming majority of trajectory events were coincident with SWR events (Sup Fig 8b). Theta power, which is high during exploration, was significantly decreased immediately before and after trajectory events (Sup Fig 8c). Collectively, these data suggest that trajectory events are functionally similar to the SWR-associated events previously reported on linear tracks as 'replay'[21–26].

## Trajectory events over-represent a known goal location

To examine whether non-local spatial information present in trajectory events contributes to or is affected by acquisition or expression of a spatial memory (the novel *HOME* location), we divided the observed trajectory events into those that were initiated while the rat was at the *HOME* location ('home-events') and those that were initiated while the rat was elsewhere ('away-events'). There was no difference in the rate of occurrence of sharp-wave/ripple events or of trajectory events between *HOME* and *RANDOM* locations (Sup Figs 9–10). As expected, home-events showed strong representation of the *HOME* location (Fig 3a,c; Fig 2c, top row), likely due to initiation bias, a tendency for hippocampal events to reflect a path that begins at the rat's current location[22–24] (butsee [25,26]). Strikingly, we observed that away-events also displayed an increased representation of the *HOME* location (Fig 3b,d; Sup Fig 11), a finding that cannot be explained through initiation bias. Consistent with this observation, many away-events depicted a trajectory that ended at *HOME* (Fig 2c, middle rows; Sup Videos 3–7). Quantification confirmed that the *HOME* location was significantly over-represented in away-events relative to other locations on the open field

Author Manuscript Author Manuscript Author Manuscript Author Manuscript

(Fig 3c, left; Sup Fig 12) and that away-events were more likely to end their trajectories at the *HOME* location than any other region of the arena (Fig 3c, center). Importantly, the region of increased representation changed accordingly when the location of the *HOME* well was moved on experimental day 2. The heightened representation of *HOME* in away-events was present even when the analysis was restricted to the first 19 trials, when the specific *RANDOM-HOME* combinations were novel (Sup Fig 13). The increased representation of *HOME* in away-events was not a simple function of increased familiarity with or time spent at the *HOME* location, as other regions of the arena with greater occupancy times did not display strong representations in trajectory events (Fig 3c, right). The over-expression of the *HOME* location in away-events could not be accounted for by either occupancy time or the spatial distribution of place fields (Sup Figs 14–15). Further, when we restricted our analysis to vectorized trajectories rather than entire posterior probabilities, the *HOME* location remained over-represented in away-events (Sup Fig 16). Thus, trajectory events in the hippocampus over-represent a known goal location in a manner which cannot be explained solely by occupancy time or place field representation.

## Trajectory events do not over-represent non-goal locations

We hypothesized that the over-representation of locations in trajectory events was selective for behaviorally relevant locations. The task was designed so that the previous *RANDOM* well was never a correct behavioral goal, and so we hypothesized in particular that the previous *RANDOM* well would not be over-represented in trajectory events. In order to equalize comparison between away-events and home-events, we rotated and scaled all home-events such that the distance and direction from the rat's physical location at the time of each event to the previously active *RANDOM* location was the same across all home-events (Fig 4a). Similarly, we rotated and scaled all away-events according to the direction and distance to the *HOME* location (Fig 4b), and as a control we rotated and scaled all home-events according to the direction and distance to the immediately future (but unknown and not yet baited) *RANDOM* well location. All rotated/scaled trajectory events displayed a strong representation of the rat's physical location (Fig 4c–e) due to initiation bias. However, while the rotated/scaled away-events displayed a strong representation of the *HOME* location (Fig 4d), rotated home-events showed little representation of the previously active (Fig 4c) or immediately-to-be active (Fig 4e) *RANDOM* locations. Indeed, we observed a significant decrease in the representation of the previous *RANDOM* location in home-events as compared to the representation of the *HOME* location in away-events (Fig 4f). These data argue that hippocampal trajectory events reflect the demands of the task by selectively over-representing the immediately relevant *HOME* location and not the irrelevant previous *RANDOM* location.

## Trajectory events reflect future behavioral path

The initiation and termination bias we observe suggests that away events depict the future trajectory to *HOME*, indicative of a planning mechanism to guide behavior. To test this hypothesis, we quantified the correspondence between trajectory events and the behavioral path in the immediate future, or immediate past (Fig 5a,b; Sup Fig 17). We calculated the angular displacement between trajectory and path at progressively increasing radii from the

Author Manuscript Author Manuscript Author Manuscript Author Manuscript

current location (Fig 5a,b). Away-events were strongly concentrated around zero angular displacement assessed against the future path, and more broadly distributed with respect to the past path (Fig 5c), and this difference was verified in terms of the mean absolute angular displacement for each event (Fig 5d). Home events showed a weaker representation of future path, and an apparent anti-correlation with past path, which might have reflected the fact that the path back to the previous *RANDOM* well was never correct (Fig 5e,f). Away-events were significantly closer to the rat's future path than were home-events (Fig 5g), consistent with the goal-directed nature of *RANDOM*-to-*HOME* navigation. We conducted two further analyses of path correspondence, one based on the orientation of the depicted trajectory to a location occupied 10s in the future or the past (Sup Fig 18), and one based on the spatial overlap between smoothed versions of the trajectory and future or past path (Sup Fig 19), with matching results. Rats displayed no bias to face the direction of their immediately future path or the *HOME* well location during away-events (Sup Fig 20a–b). Furthermore, away-events were more spatially correlated with the rat's future path than with his current heading (Sup Fig 20d–g). Thus, the strong reflection of the rat's future path in away-events could not be trivially explained as a representation of paths 'in front' of the rat, but rather suggested a more precise path-finding mechanism.

## Trajectory events actively and flexibly reflect task demands

If trajectory events reflect behavioral planning generally, they might also have depicted future behaviors when the animal did not proceed immediately to the *HOME* location. Indeed, away-events closely matched the rat's future path regardless of whether the rat's future path took it to the *HOME* location or elsewhere in the arena (Fig 6a,c). For both cases, trajectories matched the future path more than the past path (Fig 6b,d). We hypothesized that if trajectory events reflected an active process that could switch between goals, then prior to non-*HOME*-seeking behaviors, not only would the representation of the non-*HOME*-seeking path be enhanced, but the representation of the *HOME* well would be reduced. Indeed, we found reduced *HOME* representation in non-*HOME*-seeking away-events compared to *HOME*-seeking away-events (Fig 6e).

We finally hypothesized that a flexible planning mechanism should be able to specify paths of novel importance (a novel combination of start and end points) over familiar terrain. The animals' behavior showed evidence of this ability over the first 19 trials of each day. We therefore examined trajectory events during this period of each session. Away-events during this novel period also bore a strong match to the rat's future path (Fig 6f; Sup Videos 3–7), and were closer to the rat's future path than its past path (Fig 6g).

## Discussion

We have demonstrated that hippocampal SWR-associated trajectory events predict immediate future navigational behavior. This finding follows a succession of results[8] reporting that SWR-associated sequences occur robustly during the awake state[22–26], that sequences are not always facsimiles of previous behavioral episodes[22–24,26,33] and can even depict novel combinations of previous experiences[26], and that sequences can be selective to the extent of not always reporting the most recent experience[26], or even necessarily

Author Manuscript Author Manuscript Author Manuscript Author Manuscript

experiences from the current environment[25]. Moreover, disruption studies using electrical stimulation contingent on SWR detection have revealed a role for sleep SWRs in learning[34,35], and a specific role for awake SWRs in working memory but not reference memory[36], which accords with the flexibility of trajectory events in response to a daily changing goal location[27,30,31]. Regarding our observation of stronger prediction prior to goal-finding than random foraging, it is likely that during the latter behavior, an animal repeatedly makes online changes to his planned navigational trajectory, which would reduce its initial predictability. This strategic variability may be reflected in the overdispersion of place cell firing rates during random foraging[28,37]. Regarding the mechanism generating trajectory events, low-level mechanisms might have contributed, such as the spatial distributions of place cells' firing rates, although these did not account for the precise depiction of the goal location. Alternatively, it is equally possible that the spatial distributions of firing rates emerged as a consequence of the trajectory events. Simple models of encoding routes via direct experience cannot easily explain either the trial-by-trial switching of trajectory events between different goals (*HOME*-seeking versus non-*HOME*-seeking), or the trajectory events corresponding to novel *RANDOM-HOME* combinations[6,38,39], although the incorporation of contextual coding for the goal might account for some of this functionality[5,40]. It remains unknown whether trajectory events can reflect the calculation of optimal paths in more challenging navigational tasks that incorporate barriers to movement[41,42]. Finally, we might speculate on how the planning function of trajectory events operates. Trajectory depiction by place cells prior to behavior might support a plasticity mechanism that reinforces the particular path, in a way that can be accessed locally during behavior[43]. For example, trajectory events might drive associations between places *en route* and estimates of value[19,31,44,45] or chosen action[44,46] that could be accessed subsequently by local place cell activation during goal-directed behavior, perhaps in combination with a local look-ahead mechanism such as theta sequences.

In summary, our data reveal a flexible, goal-directed mechanism for the manipulation of previously acquired memories, in which behavioral trajectories to a remembered goal are depicted in the brain immediately prior to movement. Such findings address longstanding questions about the role of place cells in navigational learning and planning, as well as broader questions regarding the recall and use of stored memory. In particular, trajectory events relate to hippocampal function in multiple conceptual contexts: as a cognitive map in which routes to goals might be explored flexibly prior to behavior[1], as an episodic memory system engaging in what has been termed "mental time travel"[47], and as a substrate for the recall of imaginary events[48,49]. These conceptualizations reflect a continuity with earlier speculations on animals' capacities for inference[50]. Trajectory events offer a new experimental model for the study of these varied functions.

## Methods

### Behavior and Data Acquisition

All procedures were approved by the Johns Hopkins University Animal Care and Use Committee and followed US National Institutes of Health animal use guidelines. Behavioral

Author Manuscript Author Manuscript Author Manuscript Author Manuscript

training and in-session recording took place from late afternoon to early evening (rats were housed on a standard, noninverted, 12-hour light cycle).

Adult male Long-Evans rats (10–20 weeks old, 450–550 g) were handled daily and food-restricted to 85–90% of their free-feeding weight and then trained to traverse a 1.8 m linear track to receive a liquid chocolate-flavored reward (200 μl, Carnation) at either end. Rats were trained for the briefer of 20 minutes or 20 complete laps once per day for at least 10 consecutive days. Linear track training occurred in a room separate and visually distinct from the recording room.

After a rat achieved criterion performance on the linear track (three consecutive days with 20 laps in under 20 minutes), training on the open field was initiated in a 2 m x 2 m black arena with 30-cm-high walls and 36 identical, evenly spaced, 1.5-cm-diameter, 3-mm-deep conical reward delivery wells embedded into the floor such that the rim of each well was level with the floor (Fig 1a). Each well was attached to a tubing system that ran beneath the environment, which allowed any well to be independently and soundlessly filled or emptied by the experimenter via a hand-held syringe. During the filling of a well, no obvious visible or audible cue was available to the rat signifying that a well had been filled. When active, wells were filled with 300 μl of chocolate milk. Open field training took place in the recording room with all room and environmental cues positioned as they would be during the eventual in-session recording.

Open field training proceeded in four stages. First, each rat underwent one thirty-minute-long session per day for two days in which every available well was filled (and immediately refilled following consumption) and food crumbs were scattered throughout the arena to encourage initial exploration. This was the only stage of training in which non-liquid food was present in the arena. In the second stage of training (three days), each thirty-minute-long session began with four filled wells, one per quadrant of the arena. When the reward in one quadrant was consumed, another random well in that quadrant was filled, but only after the rat had left the quadrant and consumed reward from another quadrant. In the third stage (three days), the final experimental procedure (see below) was begun except that on the interleaved *RANDOM* trials, two randomly selected wells were filled to make the task easier to complete. When one *RANDOM* well was discovered and consumed, the second was immediately emptied and the *HOME* well was filled. Finally, on the fourth stage, the rats were trained on the final experimental protocol for the lesser of thirty minutes or for 30 trials until they reached criterion performance (30 trials in less than 30 minutes for three consecutive days). Every session began by placing the rat in one corner of the arena and then allowing free exploration.

In the final experimental protocol, the *HOME* well was initially filled and was the only filled well in the arena at the start of the session. Once the rat discovered and consumed the *HOME* well reward, a randomly selected well was filled. Only after the rat discovered and consumed the *RANDOM* well reward was the *HOME* well again filled. A trial consisted of the rat leaving the *HOME* location, discovering and consuming the reward at a *RANDOM* well and then returning to the *HOME* location and consuming the reward there. At no point in the training were the rats provided with any cue informing them when the *HOME* or a

Author Manuscript Author Manuscript Author Manuscript Author Manuscript

*RANDOM* well was filled (filling occurred during or immediately after consumption at the prior well). Instead, the rats learned to return to the *HOME* well location without cue after consuming the reward at a filled *RANDOM* well and to begin searching for a *RANDOM* well immediately after consuming the reward at *HOME*. The *HOME* well location changed every session, but was constant throughout the session. The location of the *HOME* well on the recording days had never previously been experienced by the rats as a *HOME* well location, although they had sporadically received reward in those locations as *RANDOM* wells in previous sessions.

After a rat achieved criterion performance on the task, it was surgically implanted with a microdrive array (25–30 g) containing 40 independently adjustable, gold-plated tetrodes aimed at area CA1 of dorsal hippocampus (20 tetrodes in each hemisphere; 4.00 mm posterior and 2.85 mm lateral to bregma). Following surgical implantation, tetrodes were slowly lowered into the CA1 pyramidal layer over the course of 7–10 days. Final tetrode placement and unit recording as previously described[22]. Each tetrode consisted of a twisted bundle of four 17.8 μm platinum/10% iridium wires (Neuralynx), and each wire was electroplated with gold to an impedance of <150 MOhms prior to surgery. A bone screw firmly attached to the skull served as ground. During the first four or five days following implantation, the rat was not re-exposed to the experimental arena. After this recovery time, while tetrodes were still being advanced to the hippocampus, the rat was trained once per day on the final experimental protocol for the lesser of 30 minutes or 30 trials to familiarize it with navigating the arena with the microdrive and attached wires.

All data were collected using a Neuralynx (Bozeman, MT) data acquisition system and a an overhead video system that recorded continuously at 60 Hz. The rat's position and head direction were determined via two distinctly colored, head-mounted LEDs. Analog neural signals were digitized at 32,556 Hz. Spike threshold crossings (50 μV) were recorded at 32,556 Hz. Continuous local field potential data were digitally filtered between 0.1 and 500 Hz and recorded at 3,255.6 Hz. The beginning and end of reward consumption were manually determined from the captured video data.

## Cluster Analysis

Individual units were identified by manual clustering based on spike waveform peak amplitudes using custom software (xclust2, Matt A. Wilson). Only well-isolated units were included in the analysis. Modified $L_{ratio}$ values[32] were calculated for each cluster to confirm cluster quality using the peak amplitude of each waveform as the feature set. Briefly, the $L_{ratio}$ value of cluster *C* is

$$L_{ratio} = \left( \sum_{i \notin C} (1 - CDF_{\chi^2_{df}}(D^2_{i,C})) \right) / n_s$$

where $n_s$ is the total number of spikes recorded on the tetrode throughout the experiment, $i \notin C$ is the set of spikes which are not members of cluster *C*, $D^2_{i,C}$ is the Mahalanobis distance of spike i from cluster *C*, and $CDF\chi^2_{df}$ is the cumulative distribution function of the

Author Manuscript Author Manuscript Author Manuscript Author Manuscript

$\chi^2$ distribution with *df*=4. We modified the original equation for $L_{ratio}$ to allow for comparison between tetrodes with different numbers of spikes and between experiments of varying time spans. As the original equation is a sum, even well-isolated clusters will necessarily have larger $L_{ratio}$ values for particularly long experimental sessions or if they occur on tetrodes with large numbers of spikes. Thus, we normalized the sum by the total number of spikes recorded on the tetrode.

Clustered units that may correspond to putative inhibitory neurons were excluded on the basis of spike width and mean firing rate. To ensure accurate decoding of hippocampal events, only rats in which we obtained at least 100 simultaneously recorded place units were used for subsequent analysis.

## Decoding Spatial Location

Position was binned (2 cm) and position tuning curves (place fields) were calculated as the smoothed (Gaussian kernel, st. dev. of 4 cm) histogram of firing activity normalized by the time spent per bin. Only periods of time when the rat was moving faster than 5 cm/s were used to determine place fields. Units were considered to have a place field if the unit was classified as excitatory and the peak of the tuning curve was >1 Hz.

A memoryless probability-based decoding algorithm[23] was used to estimate the rat's position throughout the experiment based upon the unit position tuning curves and the spike trains. Briefly, the probability of the animal's position (*pos*) across *M* total position bins given a time window ($\tau$) containing neural spiking (*spikes*) is

$$Pr(pos|spikes)=U/\sum_{j=1}^{M}U$$

where

$$U=\left(\prod_{i=1}^{N}f_i(pos)^{n_i}\right)e^{-T\sum_{i=1}^{N}f_i(pos)}$$

and $f_i(pos)$ is the position tuning curve of the *i*-th unit, assuming independent rates and Poisson firing statistics for all *N* units and a uniform prior over position. A time window of 250 ms was used to estimate the rat's position on a behavioral timescale. A time window of 20 ms was used to estimate position during candidate population events.

## Sequential Event Analysis

A histogram (1 ms bins) of all clustered units for times when the rat's velocity was less than 5 cm/s was smoothed (Gaussian kernel, st. dev. of 10 ms). Population events were defined as peaks in the smoothed histogram greater than the mean + 3 standard deviations. Start and end boundaries for each population event were defined as the points where the smoothed

Author Manuscript Author Manuscript Author Manuscript Author Manuscript

histogram crossed the mean. To prevent estimation artifacts, the time window boundaries for each candidate event were adjusted inward (if necessary) to ensure that the first and last estimation bins contained a minimum of 2 spikes. Candidate events in which fewer than 10% of the clustered units participated or with boundaries less than 50 ms or greater than 2000 ms apart were excluded from analysis.

For each candidate event, the rat's position was estimated using the probability-based decoding algorithm described above with a 20 ms time window, advanced in 5 ms increments throughout the putative event. Following position estimation, each candidate replay event was truncated to the longest sequence of time frames with peak posterior probability less than 20 cm from that of the previous frame. Candidate events with fewer than 10 steps in the final sequence or a start-to-end distance less than 40 cm were eliminated from future analysis. The remaining candidate events were categorized as "trajectory events". For trajectory event quantification, the posterior probabilities for every time frame of each trajectory event were summed across time. For comparison between away-events and home-events, these sums were normalized for the number of time-frames in each event. For all analyses requiring per-well quantification, the arena was sub-divided by drawing an imaginary line equidistant between each well, resulting in 36 regions, each encompassing an approximately 33 x 33 cm area (Sup Fig 4). Quantification for all event trajectory analysis in which the rat's location was not specifically examined did not include the area within 15 cm of the rat's physical location at the time of the event to avoid initiation bias.

For all trajectory events, a Monte-Carlo *P*-value was calculated using two shuffle methods: randomly shuffling cell identity and randomly shuffling each cell's place field in both the X and Y dimensions. The *P*-value was calculated as $(n+1) / (r+1)$, where $n$ is the number of shuffles that met the criteria to be classified as a trajectory event and $r$ is the total number of shuffles. 5,000 shuffles were used for both methods. All candidate events that met our criteria to be classified as trajectory events had a *P*-value less than 0.02 for both shuffle methods.

To quantify the precise spatial correlation between trajectory events and the rat's future/past path, each trajectory event was transformed into a vector of the peak posterior probabilities for each time frame of the event. Using the rat's physical location at the time of the event as the center, concentric rings were drawn around the rat with radial increments of 2 cm, starting with a radius of 15 cm. For each ring, the first crossing for the event vector and the rat's future or past path were determined and the angular displacement (the minor arc along the ring's circumference, normalized by the ring's radius) was calculated between these points. This value was compared to that obtained from 2,000 randomly selected events (chosen from across all sessions) which were spatially relocated so that the rat's physical location at the time of the random event matched the rat's physical location at the time of the trajectory event to generate a Monte-Carlo *P*-value.

### Local Field Potential Analysis

For each tetrode, one representative electrode was selected and the local field potential (LFP) signal was analyzed. To examine SWRs, the LFP was band-pass filtered between 150 and 250 Hz, and the absolute value of the Hilbert transform of this filtered signal was then

Author Manuscript Author Manuscript Author Manuscript Author Manuscript

smoothed (Gaussian kernel, SD = 12.5 ms). This processed signal was averaged across all tetrodes and ripple events were identified as local peaks with an amplitude greater than 3 SD above the mean, using only periods when the rat's velocity was less than 5 cm/sec. The start and end boundaries for each event were defined as the point when the signal crossed the mean. For theta-band power analysis, the raw LFP trace was band-pass filtered between 4 and 12 Hz and the absolute value of the Hilbert transform of the filtered signal was calculated. The z-score theta power for each electrode was determined for every timepoint of the 60 Hz position data and for 100–200 ms before and after each identified trajectory event. For power spectral density analysis, one hundred millisecond non-overlapping temporal bins were used to compute the spectrograms. A z-score was calculated for each frequency band across the entire behavioral session. The SWR or trajectory event triggered spectrograms use the peak of the ripple power or the peak of the spike density, respectively, as time zero.

## Supplementary Material

Refer to Web version on PubMed Central for supplementary material.

## Acknowledgments

This work was supported by the Alfred P. Sloan Foundation, The Brain and Behavior Research Foundation (NARSAD Young Investigator Grant) and the National Institutes of Health grant MH085823.

## References

1. O'Keefe, J.; Nadel, L. The Hippocampus As A Cognitive Map. Clarendon; 1978.
2. Morris RG, Garrud P, Rawlins JN, O'Keefe J. Place navigation impaired in rats with hippocampal lesions. Nature. 1982; 297:681–683. [PubMed: 7088155]
3. Scoville WB, Milner B. Loss of recent memory after bilateral hippocampal lesions. J Neurol Neurosurg Psychiatry. 1957; 20:11–21. [PubMed: 13406589]
4. Olton DS, Samuelson RJ. Remembrance of places past: spatial memory in rats. J Exp Psychol Anim Behav Process. 1976; 2:97–116.
5. Levy WB. A sequence predicting CA3 is a flexible associator that learns and uses context to solve hippocampal-like tasks. Hippocampus. 1996; 6:579–590. [PubMed: 9034847]
6. Redish AD, Touretzky DS. The role of the hippocampus in solving the Morris water maze. Neural Comput. 1998; 10:73–111. [PubMed: 9501505]
7. Koene RA, Gorchetchnikov A, Cannon RC, Hasselmo ME. Modeling goal-directed spatial navigation in the rat based on physiological data from the hippocampal formation. Neural Netw. 2003; 16:577–584. [PubMed: 12850010]
8. Foster DJ, Knierim JJ. Sequence learning and the role of the hippocampus in rodent navigation. Curr Opin Neurobiol. 2012; 22:294–300. [PubMed: 22226994]
9. Hok V, et al. Goal-related activity in hippocampal place cells. J Neurosci. 2007; 27:472–482. [PubMed: 17234580]
10. Wood ER, Dudchenko PA, Robitsek RJ, Eichenbaum H. Hippocampal neurons encode information about different types of memory episodes occurring in the same location. Neuron. 2000; 27:623–633. [PubMed: 11055443]
11. Ferbinteanu J, Shapiro ML. Prospective and retrospective memory coding in the hippocampus. Neuron. 2003; 40:1227–1239. [PubMed: 14687555]
12. Wilson MA, McNaughton BL. Dynamics of the hippocampal ensemble code for space. Science. 1993; 261:1055–1058. [PubMed: 8351520]

Author Manuscript Author Manuscript Author Manuscript Author Manuscript

13. O'Keefe J, Recce ML. Phase relationship between hippocampal place units and the EEG theta rhythm. Hippocampus. 1993; 3:317–330. [PubMed: 8353611]
14. Muller RU, Kubie JL. The firing of hippocampal place cells predicts the future position of freely moving rats. J Neurosci. 1989; 9:4101–4110. [PubMed: 2592993]
15. Skaggs WE, McNaughton BL, Wilson MA, Barnes CA. Theta phase precession in hippocampal neuronal populations and the compression of temporal sequences. Hippocampus. 1996; 6:149–172. [PubMed: 8797016]
16. Jensen O, Lisman JE. Hippocampal CA3 region predicts memory sequences: accounting for the phase precession of place cells. Learn Mem. 1996; 3:279–287. [PubMed: 10456097]
17. Foster DJ, Wilson MA. Hippocampal theta sequences. Hippocampus. 2007; 17:1093–1099. [PubMed: 17663452]
18. Johnson A, Redish AD. Neural ensembles in CA3 transiently encode paths forward of the animal at a decision point. J Neurosci. 2007; 27:12176–12189. [PubMed: 17989284]
19. Johnson A, van der Meer MA, Redish AD. Integrating hippocampus and striatum in decision-making. Curr Opin Neurobiol. 2007; 17:692–697. [PubMed: 18313289]
20. Louie K, Wilson MA. Temporally structured replay of awake hippocampal ensemble activity during rapid eye movement sleep. Neuron. 2001; 29:145–156. [PubMed: 11182087]
21. Lee AK, Wilson MA. Memory of sequential experience in the hippocampus during slow wave sleep. Neuron. 2002; 36:1183–1194. [PubMed: 12495631]
22. Foster DJ, Wilson MA. Reverse replay of behavioural sequences in hippocampal place cells during the awake state. Nature. 2006; 440:680–683. [PubMed: 16474382]
23. Davidson TJ, Kloosterman F, Wilson MA. Hippocampal replay of extended experience. Neuron. 2009; 63:497–507. [PubMed: 19709631]
24. Diba K, Buzsaki G. Forward and reverse hippocampal place-cell sequences during ripples. Nat Neurosci. 2007; 10:1241–1242. [PubMed: 17828259]
25. Karlsson MP, Frank LM. Awake replay of remote experiences in the hippocampus. Nat Neurosci. 2009; 12:913–918. [PubMed: 19525943]
26. Gupta AS, van der Meer MA, Touretzky DS, Redish AD. Hippocampal replay is not a simple function of experience. Neuron. 2010; 65:695–705. [PubMed: 20223204]
27. Steele RJ, Morris RG. Delay-dependent impairment of a matching-to-place task with chronic and intrahippocampal infusion of the NMDA-antagonist D-AP5. Hippocampus. 1999; 9:118–136. [PubMed: 10226773]
28. Olypher AV, Lansky P, Fenton AA. Properties of the extra-positional signal in hippocampal place cell discharge derived from the overdispersion in location-specific firing. Neuroscience. 2002; 111:553–566. [PubMed: 12031343]
29. Kentros CG, Agnihotri NT, Streater S, Hawkins RD, Kandel ER. Increased attention to spatial context increases both place field stability and spatial memory. Neuron. 2004; 42:283–295. [PubMed: 15091343]
30. Eichenbaum H, Otto T, Cohen NJ. The hippocampus--what does it do? Behav Neural Biol. 1992; 57:2–36. [PubMed: 1567331]
31. Foster DJ, Morris RG, Dayan P. A model of hippocampally dependent navigation, using the temporal difference learning rule. Hippocampus. 2000; 10:1–16. [PubMed: 10706212]
32. Schmitzer-Torbert N, Jackson J, Henze D, Harris K, Redish AD. Quantitative measures of cluster quality for use in extracellular recordings. Neuroscience. 2005; 131:1–11. [PubMed: 15680687]
33. Csicsvari J, O'Neill J, Allen K, Senior T. Place-selective firing contributes to the reverse-order reactivation of CA1 pyramidal cells during sharp waves in open-field exploration. Eur J Neurosci. 2007; 26:704–716. [PubMed: 17651429]
34. Girardeau G, Benchenane K, Wiener SI, Buzsaki G, Zugaro MB. Selective suppression of hippocampal ripples impairs spatial memory. Nat Neurosci. 2009; 12:1222–1223. [PubMed: 19749750]
35. Ego-Stengel V, Wilson MA. Disruption of ripple-associated hippocampal activity during rest impairs spatial learning in the rat. Hippocampus. 2010; 20:1–10. [PubMed: 19816984]

Author Manuscript Author Manuscript Author Manuscript Author Manuscript

36. Jadhav SP, Kemere C, German PW, Frank LM. Awake Hippocampal Sharp-Wave Ripples Support Spatial Memory. Science. 2012

37. Jackson J, Redish AD. Network dynamics of hippocampal cell-assemblies resemble multiple spatial maps within single tasks. Hippocampus. 2007; 17:1209–1229. [PubMed: 17764083]

38. Buzsaki G. Two-stage model of memory trace formation: a role for "noisy" brain states. Neuroscience. 1989; 31:551–570. [PubMed: 2687720]

39. Mehta MR, Lee AK, Wilson MA. Role of experience and oscillations in transforming a rate code into a temporal code. Nature. 2002; 417:741–746. [PubMed: 12066185]

40. Gerstner W, Abbott LF. Learning navigational maps through potentiation and modulation of hippocampal place cells. Journal of computational neuroscience. 1997; 4:79–94. [PubMed: 9046453]

41. Poucet B, Thinusblanc C, Chapuis N. Route Planning in Cats, in Relation to the Visibility of the Goal. Anim Behav. 1983; 31:594–599.

42. Foster D, Dayan P. Structure in the space of value functions. Machine Learning. 2002; 49:325–346.

43. Sutton, RS. Neural Networks for Control. Miller, T.; Sutton, RS.; Werbos, P., editors. MIT Press; 1990.

44. Montague PR, Dayan P, Sejnowski TJ. A framework for mesencephalic dopamine systems based on predictive Hebbian learning. J Neurosci. 1996; 16:1936–1947. [PubMed: 8774460]

45. Lansink CS, Goltstein PM, Lankelma JV, McNaughton BL, Pennartz CM. Hippocampus leads ventral striatum in replay of place-reward information. PLoS Biol. 2009; 7:e1000173. [PubMed: 19688032]

46. van der Meer MA, Johnson A, Schmitzer-Torbert NC, Redish AD. Triple dissociation of information processing in dorsal striatum, ventral striatum, and hippocampus on a learned spatial decision task. Neuron. 2010; 67:25–32. [PubMed: 20624589]

47. Tulving E. Episodic memory: from mind to brain. Annual review of psychology. 2002; 53:1–25.

48. Hassabis D, Kumaran D, Vann SD, Maguire EA. Patients with hippocampal amnesia cannot imagine new experiences. Proc Natl Acad Sci U S A. 2007; 104:1726–1731. [PubMed: 17229836]

49. Buckner RL. The role of the hippocampus in prediction and imagination. Annual review of psychology. 2010; 61:27–48. C21–28.

50. Tolman, E. Purposive behavior in animals and men. The Century Co; 1932.

Author Manuscript Author Manuscript Author Manuscript Author Manuscript

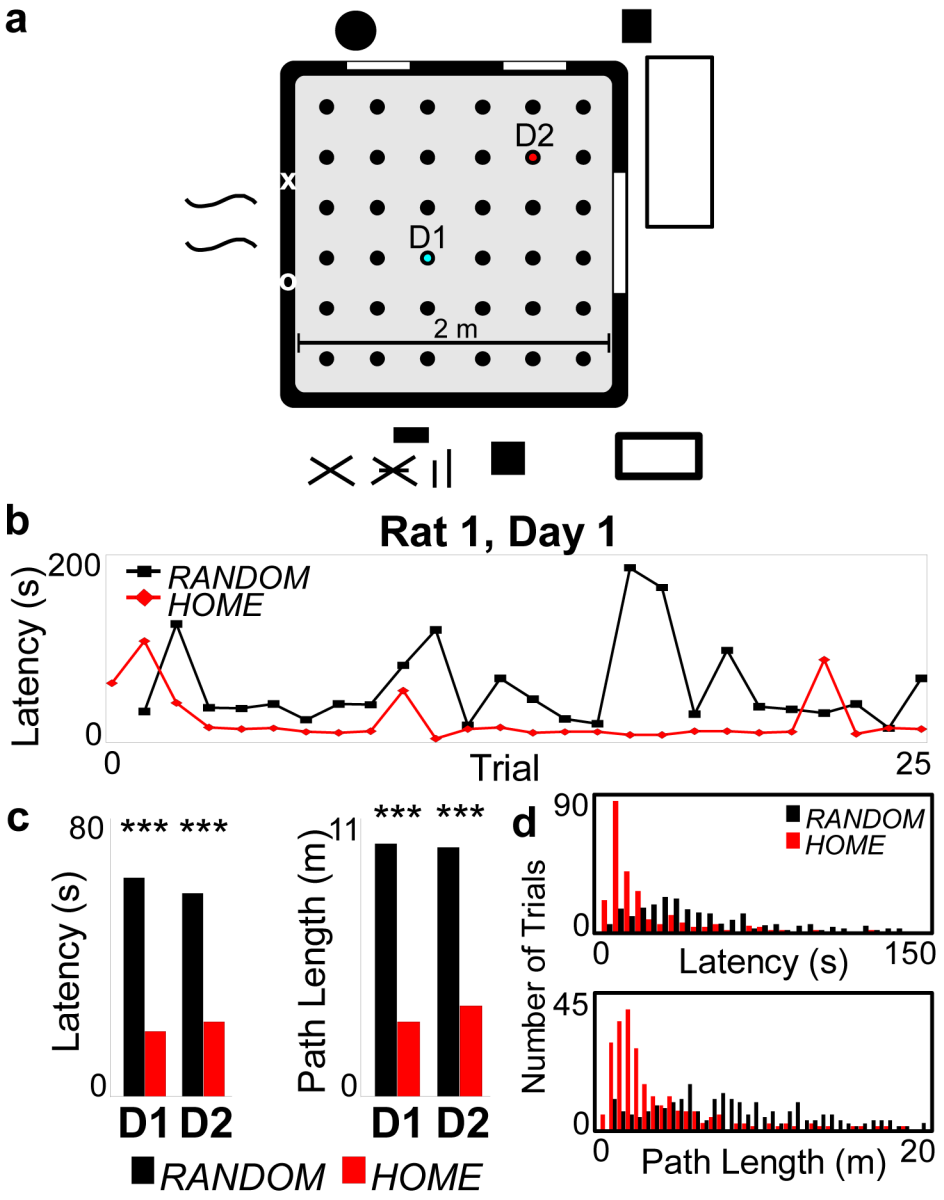


**Figure 1. Behavior in the open-field spatial memory task**

**a,** Schema of arena and room, reward wells (circles), and *HOME* location for days 1 and 2 (D1, cyan; D2, red). **b,** Per-trial latency to reach *HOME* or *RANDOM* well location for rat 1 (R1) on D1. **c,** Mean latency and path length to reach *HOME* or *RANDOM* well location across all rats for D1 and D2. *P*-values (Wilcoxon rank sum test): Latency D1 $5.5 \times 10^{-19}$, D2 $9.7 \times 10^{-14}$; Path D1 $2.7 \times 10^{-19}$, D2 $5.2 \times 10^{-16}$. **d,** Histogram of latencies (5 s bins) and path lengths (50 cm bins) for all trials (shown to 150s and 20m respectively) *P*-values (Kolmogorov-Smirnov test): Latency $2.6 \times 10^{-2}$; Path $9.1 \times 10^{-4}$.

Author Manuscript Author Manuscript Author Manuscript Author Manuscript

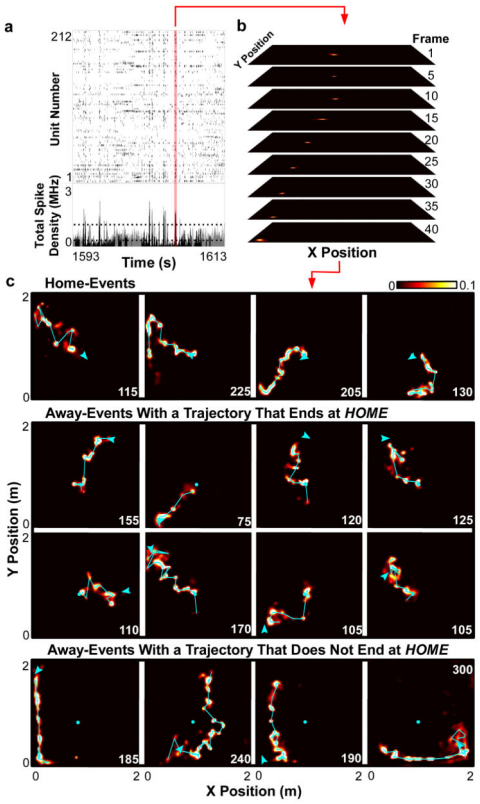


**Figure 2. Trajectory events**

**a,** Raster plot (top) and spike density (bottom) of simultaneous unit activity for R1,D1 for representative epoch. Periods of immobility denoted in black. Dashed lines represent candidate event detection threshold. **b,** Position posterior probabilities in selected frames for the candidate event in **a. c,** 16 representative events (of 274) for R1,D1, decoded and summed across time. Values indicated by colorbar. Event duration (in ms) in right corner. Cyan circle: *HOME* well. Cyan line: peak probability for each timeframe. Cyan arrowhead: position and head direction of rat at time of event. Videos of each event available in online SupplementaryVideo 2.

Author Manuscript Author Manuscript Author Manuscript Author Manuscript

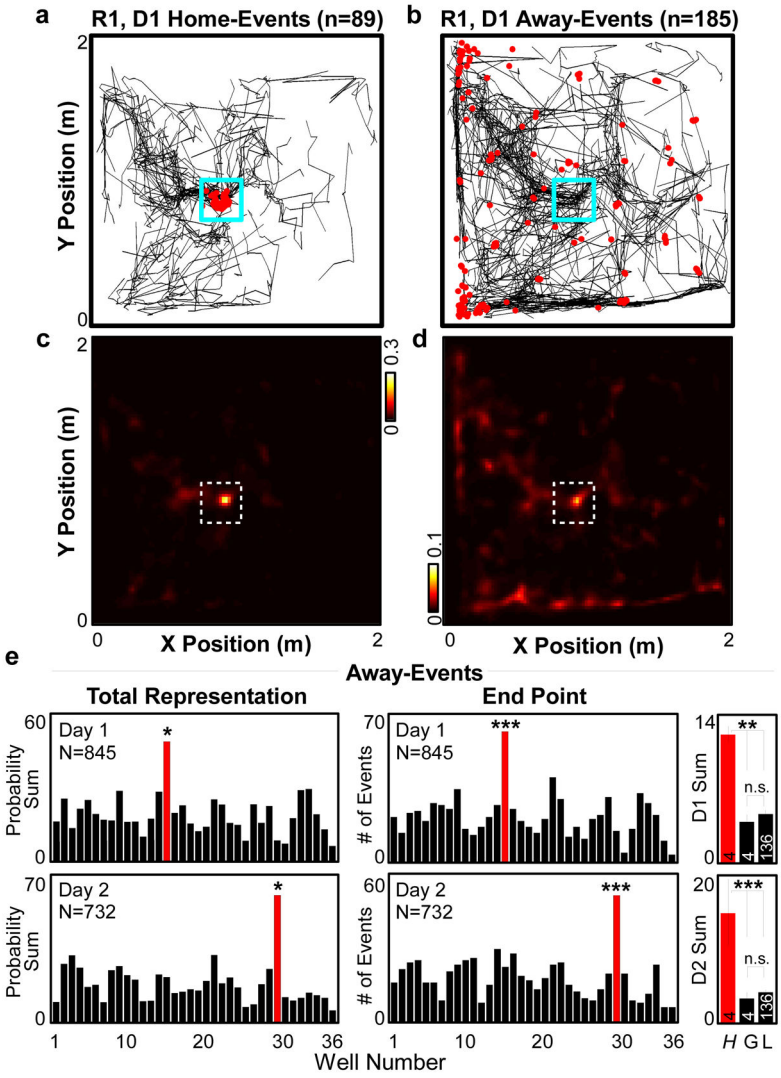


**Figure 3. Remote representation of goal location**

**a–d,** Vectorized trajectories (**a,b**) and average posterior probability sum (**c,d**) of all confirmed home-events (left) and away-events (right) for R1,D1. Red dots in **a,b**: rat location at time of event. Dashed box in **c,d**: *HOME* location. **e,** Left, Posterior probability sum for all away-events across all rats. *HOME* (red) is a statistical outlier. *P*-value (Grubbs' test for outliers): *D1* $2.3\text{x}10^{-2}$ (Lilliefors test, *P*-value 0.15); D2 $1.1\text{x}10^{-2}$ (Lilliefors *P*-value 0.32). Center, Number of away-events across all rats in which the final frame peak posterior probability was at each well. *HOME* (red) is a statistical outlier. *P*-values (Grubbs' test for outliers): D1 $6.9\text{x}10^{-4}$ (Lilliefors test, *P*-value 0.29); D2 $6.0\text{x}10^{-4}$ (Lilliefors *P*-value 0.42). Right, as left, but mean ± s.e.m. for *HOME* (*H*), all wells with greater in-session total occupancy than *HOME* (G), and all wells with less occupancy than *HOME* (L). *P*-values (ANOVA, Tukey-Kramer post-hoc multiple comparison): D1 *H* vs. G $2.9\text{x}10^{-3}$, *H* vs. L $8.5\text{x}10^{-5}$, G vs. L 0.91; D2 *H* vs. G $7.4\text{x}10^{-8}$, *H* vs. L $<1\text{x}10^{-10}$, G vs. L 0.82.

Author Manuscript Author Manuscript Author Manuscript Author Manuscript

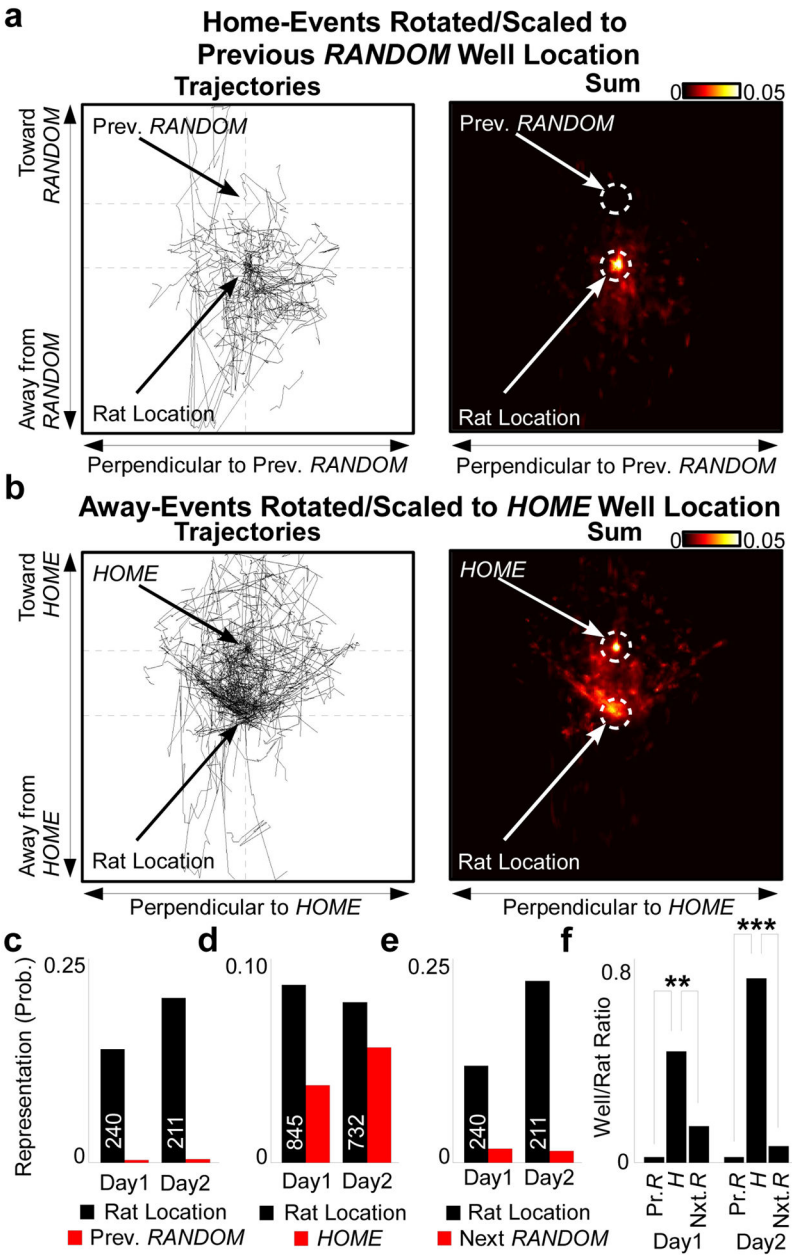


**Figure 4. Representation of relevant vs. irrelevant locations**

**a,** Vectorized trajectories (left) and average posterior probability sum (right) of all home-events for R1,D1, centered by rat's physical location at time of event and rotated and scaled according to direction and distance to the previously rewarded *RANDOM* location. White circles: quantified regions. **b,** As **a**, for *HOME*. **c–e,** Across all rats, mean representation of quantified regions as in **a–b**. Event number displayed on bar. **f,** Normalized ratio of well/rat representation for **c–e**. *P*-values (Wilcoxon rank sum test): D1 *HOME* vs. Prev. *RANDOM* $4.4\text{x}10^{-16}$, *HOME* vs. Next *RANDOM* $9.9\text{x}10^{-3}$; D2 *HOME* vs. Prev. *RANDOM* $3.1\text{x}10^{-20}$, *HOME* vs. Next *RANDOM* $1.3\text{x}10^{-13}$.

Author Manuscript Author Manuscript Author Manuscript Author Manuscript

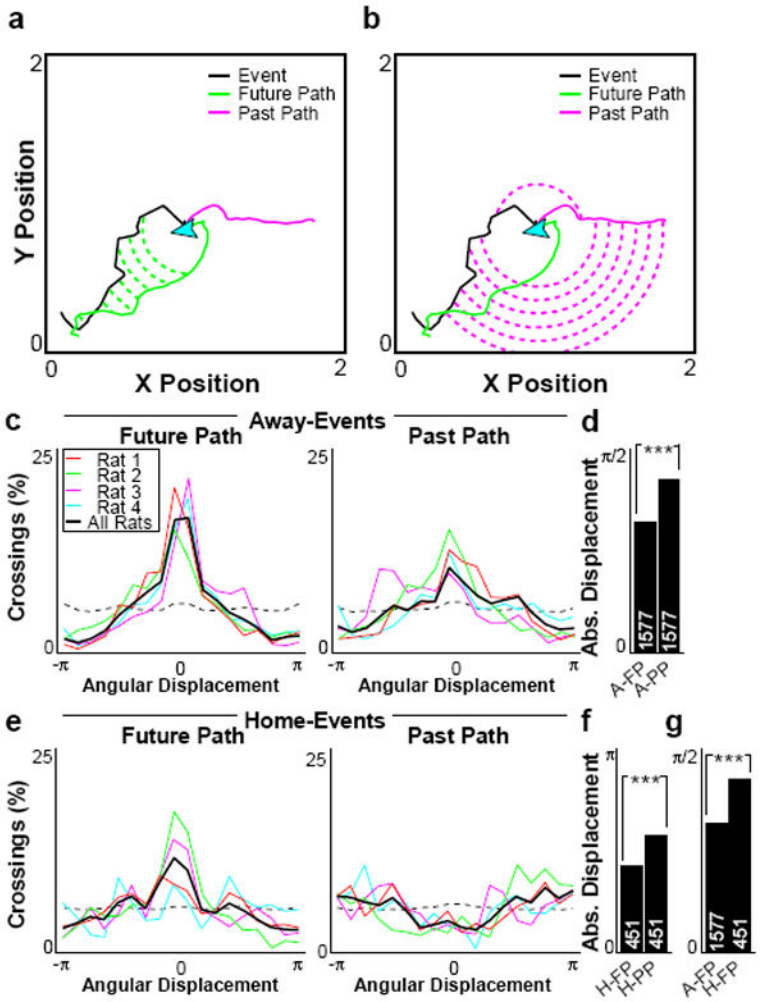


**Figure 5. Correspondence to past or future path**

**a–b,** Representative event from R1, D1, demonstrating trajectory event vector (black), immediate future (green) and past (magenta) path (up to greater of 10 s or 50 cm), and angular displacement along the minor arc between event and future (**a**) or past (**b**) path at each crossing. **c,** Percent of crossings across all events as a function of angular displacement for all away-events compared to future (left) or past (right) path. Dashed line indicates chance based upon 2,000 shuffled events. **d,** Mean absolute angular displacement for away-events compared to future (A-FP) or past (A-PP) path. **e–f,** As **c–d**, for home-events. **g,** Mean absolute angular displacement for future path for all away-events (A-FP) or home-events (H-FP). *P*-values (Wilcoxon rank-sum test): **d**) $8.60 \times 10^{-31}$; **f**) $3.54 \times 10^{-17}$; **g**) $7.25 \times 10^{-16}$.

Author Manuscript Author Manuscript Author Manuscript Author Manuscript

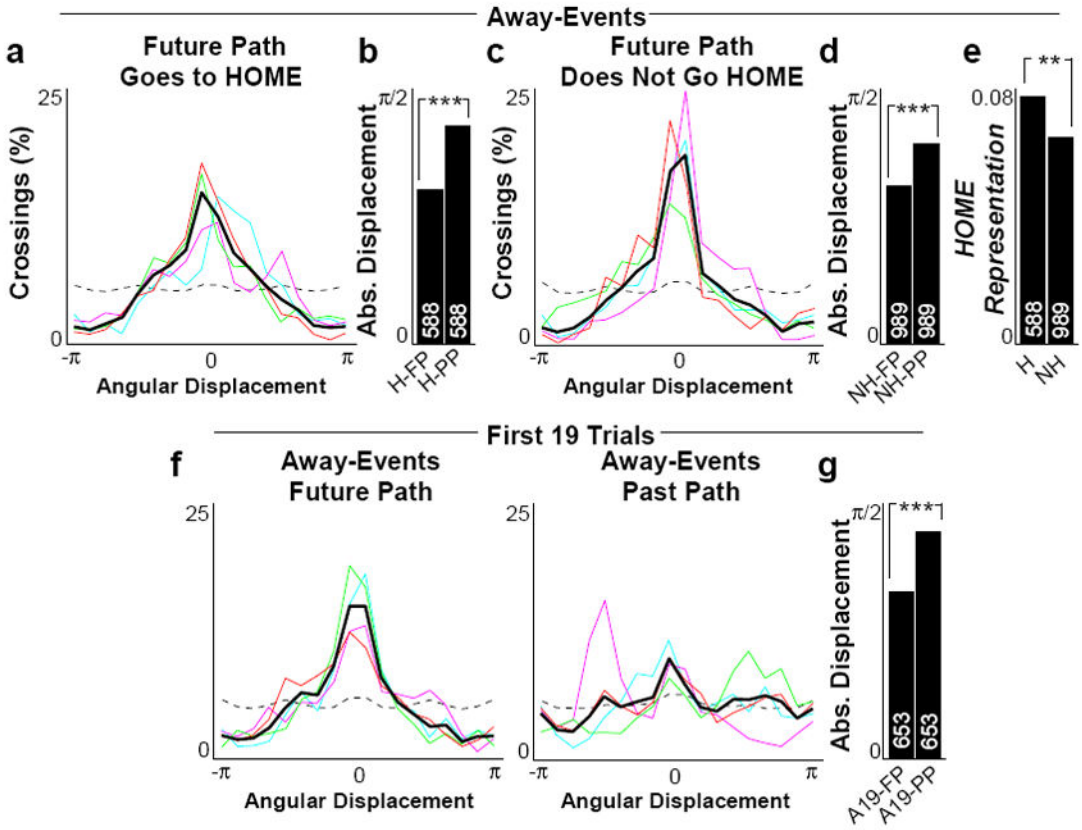


**Figure 6. Goal switching and flexibility in trajectory events**

**a–b,** As Figure 5c (left) and **5d**, for away-events preceding behavior ending at or crossing *HOME* (future path, H-FP; past path, H-PP). **c–d,** As **a–b**, for away-events preceding behaviors directed elsewhere. **e,** Mean posterior probability representation of *HOME* for same division of away-events (to *HOME*, H; not to *HOME*, NH). **f–g**, As **5c–d**, for away-events from the first 19 trials of each session (future path, A19-FP; past path, A19-PP). *P*-values (Wilcoxon rank-sum test): **b**) $4.96 \times 10^{-22}$; **d**) $1.12 \times 10^{-13}$; **e**) $9.60 \times 10^{-3}$; **g**) $2.37 \times 10^{-10}$.